Journal of Applied Electrochemistry (2005) 35:967–973
DOI 10.1007/s10800-005-6723-0

Electrochemical oxidation of ferulic acid in aqueous solutions at gold oxide and lead dioxide electrodes

S. KALLEL TRABELSI, N. BELHADJ TAHAR, B. TRABELSI and R. ABDELHEDI*
UR Electrochimie et Environnement, Ecole Nationale d'Ingénieurs de Sfax, BPW, 3038, Sfax, Tunisie
*(*author for correspondence, e-mail: Ridha.Abdelhedi@enis.rnu.tn)*

Received 6 May 2004; accepted in revised form 18 April 2005

Key words: anodic oxidation, ferulic acid, gold electrode, lead dioxide, wastewaters treatment

Abstract

A kinetic study of the electrochemical oxidation of ferulic acid (3-methoxy-4-hydroxycinnamic acid) by direct electron transfer at treated gold disk was combined with results of electrolyses in order to produce total degradation into CO_2 and H_2O at Ta/PbO_2 anode. The oxidation of ferulic acid at gold electrode was studied by cyclic voltammetry. At low concentration, ferulic acid shows one irreversible anodic peak. The peak current shows adsorption characteristics. For ferulic acid concentrations higher than 0.02 mmol dm^{-3}, the voltammogram shows two anodic peaks. The effect of experimental conditions on the ratio of these two peaks was examined. The proposed mechanism is based on the hypothesis of two-electron oxidation of ferulic acid molecule involving a three intermediate cation mesomers. Hydrolysis of these mesomers leads to the formation of caffeic acid, methoxyhydroquinone and 3,4-dihydroxy-5-methoxycinnamic acid. Then ferulic acid was quantitatively oxidised by electrolysis on lead dioxide to produce, via intermediate aromatic compounds, maleic acid, oxalic acid and formic acid whose oxidation leads to carbon dioxide.

1. Introduction

Wastewaters from the olive oil industry are a very serious problem owing to the fact that they are not easily biodegradable [1]. Ferulic acid is a contaminant present in these wastewaters [2].

Oxidation of ferulic acid has been the subject of many studies [3–7]. The enzymatic oxidation of ferulic acid by laccase produces, via three intermediate radical mesomers, two major products having a dimeric structure [3]. Chemical oxidation of ferulic acid was studied by Fenton's reagent and a kinetic model was applied to calculate the rate constant [4]. Ozonisation of ferulic acid was studied under different experimental conditions such as pH and temperature in order to obtain kinetic data [5]. Miranda et al. [6] have shown that in acid and basic media, ozone is able to oxidise ferulic acid into smaller compounds where oxalic acid is the main oxidation intermediate while vanillin, vanillic and maleic acids reach only lower concentrations. They suggested a global mechanism involving exocyclic double bond cleavage, hydroxylation and cleavage of the aromatic ring.

Electrochemical oxidation by cyclic voltammetry at glassy carbon and gold electrodes was studied in water and in several water and organic solvents mixtures [7]. The cyclic voltammetry of ferulic acid was investigated at different pH values in 50/50 water + methanol mixtures. At neutral or slightly acidic pH, the value of the peak potential varies linearly with the pH. At higher pH, it remains constant up to pH = 13. The proposed mechanism involved a fast one-electron transfer followed by an irreversible coupling of two phenoxy radicals according to a second-order rate law.

In this work, we have studied the electrochemical behaviour of ferulic acid aqueous solutions by cyclic voltammetry at gold oxides electrodes. The kinetics of the first stages which precede the opening of the aromatic ring in the oxidation mechanism of ferulic acid was investigated.

Gold was often regarded as the ideal solid electrode for fundamental electrochemical investigation as this metal does not allow the aromatic compounds to degrade effectively. However, the complete degradation of such compounds can be done only on electrode materials characterised by a high oxygen over-potential such as PbO_2 [8–13], SnO_2 [14, 15], diamond [16] and boron – doped diamond [17–19]. In the second part of this work, we will use a Ta/PbO_2 anode in order to degrade ferulic acid into smaller and more easily biodegradable compounds. It should be noted that at low anodic potential, PbO_2 behaves like gold vis-à-vis the aromatic compounds oxidation [20].

2. Experimental details

2.1. *Apparatus*

Cyclic voltammograms were recorded using a GSTP4 Tacussel X-Y recorder. Potential control of the working electrode was achieved using a Tacussel potensiostat (model PJT). The charge was measured by a Tacussel integrator (IG6N type). The reference electrode was the saturated mercurous sulphate (standard potential $E^0 = 0.61$ V/SHE).

The electrolysis products were assayed by liquid chromatography (Hewlett Packard 1100) with the aid of a Hamilton PRP X 300 column specifically for organic acids [9, 13]. The mobile phase was a mixture of methanol and 5×10^{-2} mol dm^{-3} sulfuric acid solution with the percentage by volume of methanol varying linearly with time as follows: from 2 to 20% for the first 10 minutes then from 20 to 40% up to 20 min and from 40 to 60% up to 40 min and finally from 60 to 80% up to 50 minutes.

The total organic carbon (TOC) was measured using a Shimadzu TOC analyser. Complementary details for electrolysis and analysis are given in reference [21].

2.2. *Reagents*

All the reagents used in this study were of analytical grade acquired from Aldrich. They were used without previous purification. All solutions were prepared using doubly distilled water.

2.3. *Treatment of gold electrode*

The working electrode was a polycrystalline gold disk of ca. 0.0314 cm^2 exposed area. This electrode was mechanically polished with a fine alumina powder ($\phi = 0.3\mu$m) and washed with doubly distilled water before transfer to the cell. The electrode was then subjected to potential cycling conditions, in sulphuric acid (0.5 mol dm^{-3}), between -0.61 and $+0.19$ V vs. a saturated mercurous sulphate at a scan rate of 5 V s^{-1} for a period depending on the desired oxide layer thickness. The initially bright gold electrode became red brown. The electrochemical response of the treated electrode is presented on Figure 1 (curve 1). The cyclic voltammogram was characterised by a large peak beginning at $+0.70$ V and corresponding to the gold electro-oxidation while the reduction peak of the gold oxides was observed at $+0.54$ V. The gold oxide electrode was characterised by the charge Q corresponding to the electrochemical formation of the gold oxides [22]. Q was considered as the main characteristic of the electro-active surface.

2.4. *Preparation of Ta/PbO_2 electrode*

The electrode used for large-scale electrolyses was made of tantalum rectangular plates (70 mm $\times$ 10 mm $\times$ 1 mm) covered with a layer of lead dioxide obtained by electrochemical oxidation of lead nitrate aqueous solution. In order to obtain a rough substrate surface to ensure the adhesion of PbO_2 deposits, the tantalum plates underwent sandblasting using silica grains with an average diameter of 0.3 mm projected under 5 bar pressure. The substrate was then ultrasonically rinsed in doubly distilled water and chemically etched with HF 40% (weight) for 30 s at room temperature. The lead dioxide was then galvanostatically deposited using a two compartment cell ($V = 200$ cm^3) containing a lead nitrate solution (1 mol dm^{-3}). The cathode was a bar of graphite ($\phi = 1$ cm, $L = 6$ cm) placed in a porous ceramic cylinder (Norton, Refractaire RA 84) containing 1 mol dm^{-3} sulphuric acid solution. The deposition of PbO_2 was carried out for 2.5 h, at 65 °C and using an anodic current density of 20 mA cm^{-2}. The average mass of PbO_2 deposited per unit of surface area was 0.22 g cm^{-2}. The deposit obtained was mat grey and adherent.

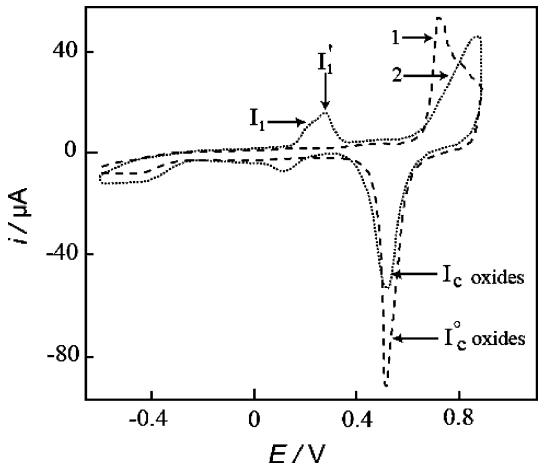

Fig. 1. Cyclic voltamograms of ferulic acid at gold disk ($\phi = 1$ mm, $Q = 0.25$ mC) in 0.5 mol dm^{-3} sulphuric acid aqueous solution. $v = 50$ mV s^{-1}; $T = 20$ °C. Key: ferulic acid concentration: (1) 0; (2) 0.5 mmol dm^{-3}.

2.5. *Electrolyses*

The electrolyses of ferulic acid aqueous solutions were carried out in an isothermal reactor with two compartments. The electrolytic solution treated ($V = 140$ cm^3) initially contained ferulic acid (0.5 mmol dm^{-3}) in H_2SO_4 (pH = 2). The Ta/PbO_2 anode was made up of two identical plates placed symmetrically around the cathode; the opposite face of each plate relative to the cathode was masked with a protective film (transparent polyethylene tape, Scotch TM 480. 3 M). The total surface area of the working electrode was 10 cm^2. The cathode was a bar of graphite ($\phi = 1$ cm, $L = 6$ cm) placed in a porous ceramic cylinder (Norton, Refractaire RA 84) containing 1 mol dm^{-3} sulphuric acid solution. The acid solutions of ferulic acid were electrolysed at 65 °C, with magnetic stirring and under a constant anodic current density of 12 mA cm^{-2}.

3. Results and discussion

3.1. *Voltammetric study*

The oxidation of ferulic acid was first studied by cyclic voltammetry at treated gold electrode. A typical voltammogram for the oxidation of 0.5 mmol dm^{-3} ferulic acid solution in sulphuric acid (0.5 mol dm^{-3}) at a scan rate of 50 mV s^{-1} is shown in Figure 1 (curve 2). During the first forward positive scan, ferulic acid shows two anodic peaks I_1 and I_1' at 240 and 270 mV, respectively. On the reverse scan, a broad reduction peak is visible at 150 mV. The electrochemical behaviour of ferulic acid aqueous solution was studied as a function of its concentration, the Q value, the potential scan rate and the solvent composition.

3.1.1. *Influence of ferulic acid concentration*

Figure 2 shows some cyclic voltammograms recorded at treated gold electrode characterised by a Q value of 0.25 mC in ferulic acid aqueous solution at concentrations ranging from 0.02 to 0.5 mmol dm^{-3}. For ferulic acid concentrations less than 0.02 mmol dm^{-3}, only the peak I_1' is visible. With increasing ferulic acid concentration above 0.02 mmol dm^{-3}, peak I_1 appears. The current of the latter ($i_p(I_1)$) rises linearly with ferulic acid concentration, while that of peak $I_1'(i_p(I_1'))$ increases linearly up to 0.02 mmol dm^{-3} then tends to stabilise around 2 μA (Figure 3).

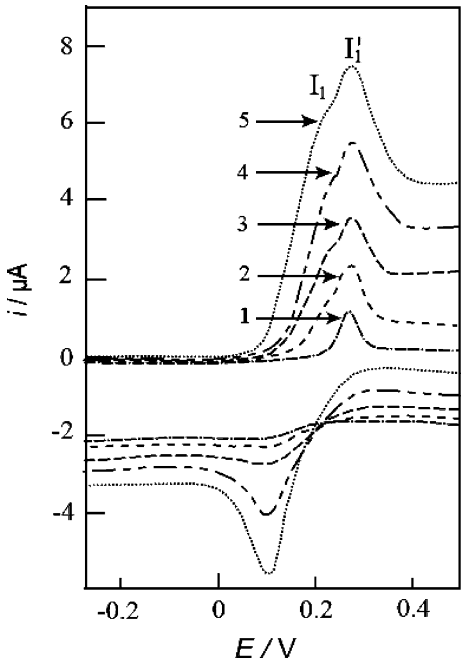

Fig. 2. Cyclic voltamograms of ferulic acid at gold disk (ϕ = 1 mm, Q = 0.25 mC) in 0.5 mol dm^{-3} sulphuric acid aqueous solution. v = 20 mV s^{-1}; T = 20 °C. Key: ferulic acid concentration: (1) 0.02; (2) 0.1; (3) 0.2; (4) 0.3; (5) 0.5 mmol dm^{-3}.

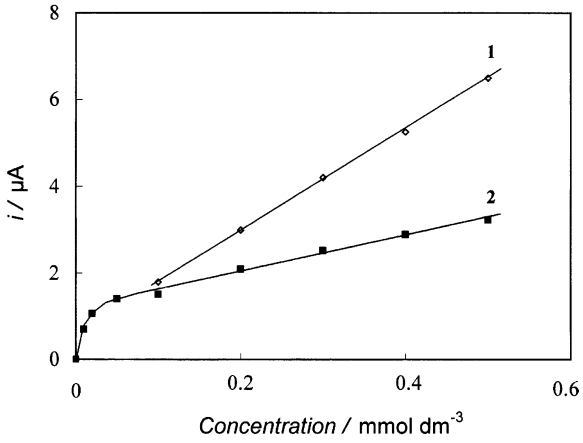

Fig. 3. Variation of the current of the peaks I_1 and I_1' as a function of ferulic acid concentration. Same conditions as in Figure 2. Key: (1) $i_p(I_1)$; (2) $i_p(I_1')$.

3.1.2. *Influence of the charge (Q)*

Figure 4 shows some cyclic voltammograms in 0.5 mmol dm^{-3} ferulic acid aqueous solution at treated gold electrodes characterised by Q values in the range 0.15–0.50 mC. The currents $i_p(I_1)$ and $i_p(I_1')$ increase linearly with the value of Q (Figure 5).

If we name $i_p(I_c^\circ)_{oxides}$ and i_p $(I_c)_{oxides}$ the reduction current of the Au oxide layer, respectively in the absence and the presence of ferulic acid, the degree of coverage θ can be calculated by the following formula [22]:

$$\theta = 1 - (i_p(I_c)_{oxides}/i_p(I_c^\circ)_{oxides}) \quad (1)$$

As can be seen from (Figure 5, curve 3) the degree of coverage θ decreases as a function of Q.

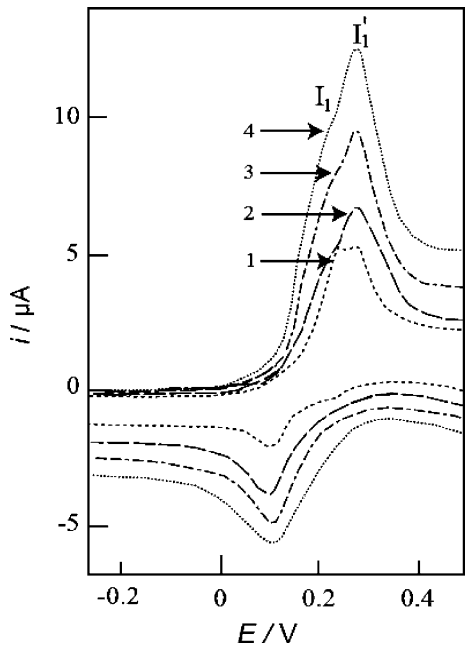

Fig. 4. Cyclic voltamograms of ferulic acid (0.5 mmol dm^{-3}) at gold disk in sulphuric acid aqueous solution. Other conditions as in Figure 2. Key: Q: (1) 0.15; (2) 0.25; (3) 0.35; (4) 0.48 mC.

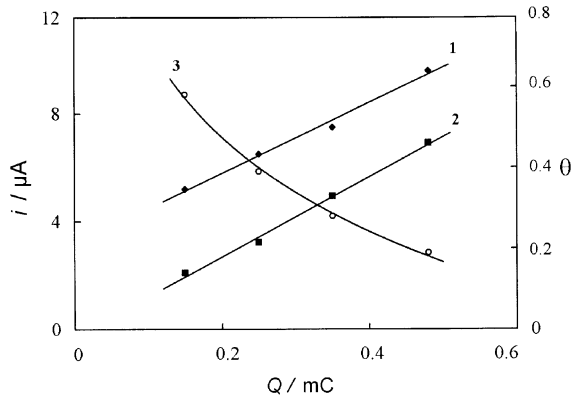

Fig. 5. Variation of the current of the peaks I_1 and I_1' and the degree of coverage θ as a function of the charge Q. Same conditions as in Figure 4. Key: (1) $i_p(I_1)$; (2) $i_p(I_1')$; (3) θ.

3.1.3. *Influence of the solvent nature*

The oxidation of ferulic acid was studied by cyclic voltammetry in several water + acetone mixtures 0.5 mol dm^{-3} H_2SO_4. By increasing the volumetric fraction of acetone, the potentials of the peaks I_1 and I_1' become gradually more positive. For 30% of acetone, the voltammogram presents peak I_1 alone; the peak I_1' disappears (Figure 6). The voltammograms show that the current $i_p(I_1)$ decreases as water is substituted by acetone. In water + acetone mixture (30/70 vol.), the peak I_1' reappears for ferulic acid concentration higher than 1 mmol dm^{-3}.

3.1.4. *Influence of the potential scan rate*

From voltammograms presented in Figure 7, we have shown that the current $i_p(I_1)$ varies linearly with the square root of the potential scan rate v. The slope of the straight line representing $i_p(I_1)$ as a function of the

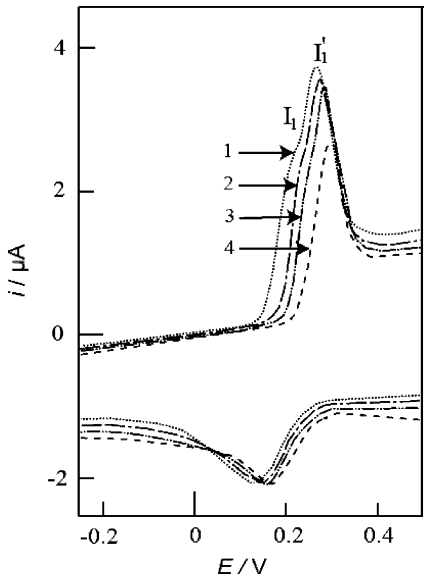

Fig. 6. Cyclic voltamograms of ferulic acid (0.2 mmol dm^{-3}) at gold disk in mixtures of water and acetone. Other conditions as in Figure 2. Key: volumetric fraction of acetone: (1) 0; (2) 10; (3) 20; (4) 30%.

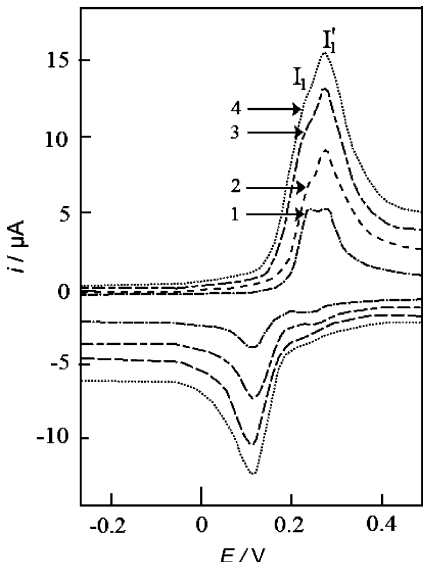

Fig. 7. Cyclic voltamograms of ferulic acid (0.5 mmol dm^{-3}) at gold disk (Q = 0.15 mC) in sulphuric acid aqueous solution. Other conditions as in Figure 2. Key: potential scan rate: (1) 20; (2) 50; (3) 80; (4) 100 mV s^{-1}.

square root of the potential scan rate v gives the diffusion coefficient D of ferulic acid by application of the equation:

$$i_p(I_1) = 2.69 \times 10^5 n^{3/2} S D^{1/2} v^{1/2} C \qquad (2)$$

where n is the number of exchanged electrons; S is the electrode surface area (cm^2); D is diffusion coeffiecient (cm^2 s^{-1}); v is the scan rate (V s^{-1}); and C is the ferulic acid concentration (mol cm^{-3})

The diffusion coefficient of ferulic acid, calculated for n = 2, is 7.05×10^{-6} cm^2 s^{-1} at 25 °C. Although to our knowledge this diffusion coefficient has not previously been estimated, its value found in this work is situated in the range of compounds having a similar structure which undergo a first bielectronic discharge [23].

On the other hand, the voltammograms shown in Figure 7 show that when the potential scan rate increases, $i_p(I_1')$ rises more than $i_p(I_1)$. When the ferulic acid concentration is less than 0.02 mmol dm^{-3}, only the anodic peak I_1' is observed and its current varies proportionally with the potential scan rate.

3.1.5. *Discussion*

The results presented above may be interpreted by assuming that the electrochemical oxidation of ferulic acid molecules takes place on the treated gold electrode by electron transfer for both free and adsorbed forms. The free form corresponds to the first peak I_1 while the strongly adsorbed form, which is consequently stabilised, is oxidised at a more anodic potential and corresponds to the "post-peak" I_1'.

The adsorption aspect of the peak I_1' is confirmed according to the procedure already undertaken in previous studies in the case of the oxidation of phenol at platinum [24]. The treated gold electrode is immersed into ferulic acid aqueous solution then rinsed in doubly

Table 1. Variation of the quotient $i_p(I_1')/i_p(I_1)$ as a funnction of ferulic acid concentration.

[Ferulic acid]/mM	$i_p(I_1')/i_p(I_1)$
0.05	0.79
0.1	0.69
0.2	0.66
0.3	0.64
0.4	0.56
0.5	0.51

Same conditions in Figure 2.

distilled water and immediately subjected to potential cycling in 0.5 mol dm^{-3} sulphuric acid aqueous solution. The voltammogram shows only a single anodic peak which appears towards 240 mV. This peak which results from the oxidation of the adsorbed ferulic acid coincides with the peak I_1'. Its current intensity varies linearly with potential scan rate v according to the equation:

$$i_p(I_1')_{ads} = \frac{n^2F^2}{4RT} \cdot Sv\Gamma \qquad (3)$$

where Γ is the superficial concentration (mol cm^{-2}) of adsorbed ferulic acid.

Table 1 shows that the quotient $I_p(I_1')/I_p(I_1)$ decreases as ferulic acid concentration increases. Therefore, we have verified that the equilibrium between the free and adsorbed forms was quickly reached so that the quotient $i_p(I_1')/i_p(I_1)$ is not sensitive to the time lapse between the introduction of the electrode to the ferulic acid solution and the moment of potential scanning.

At very low concentrations, only the post-peak is observed. As the ferulic acid concentration increases, the post-peak current $i_p(I_1')$ increases, reaching a limiting value which corresponds to the limiting value of Γ (Figure 3, curve 2). In these conditions, the diffusion current $i_p(I_1)$ rises linearly as a function of the concentration (Figure 3, curve 1). As a consequence, the oxidation of dissolved ferulic acid presumably occurs either through the adsorbed ferulic acid film or at the free surface as was demonstrated in previous work [15].

The disappearance of post-peak I_1' when water is substituted by acetone can be explained by the predominant adsorption of acetone on gold, gradually inhibiting the adsorption of ferulic acid as acetone content increases.

3.1.6. *Identification of oxidation products*

Figure 8 shows successive cyclic voltammograms of 0.5 mmol dm^{-3} ferulic acid solution at a gold disk characterised by a Q value of 0.25 mC. From the second cycle, the voltammograms show the appearance of three other reversible peaks I_2, I_3 and I_4 situated, respectively, at −0.1, 0 and 0.15 V. The peaks I_2 and I_4, are respectively ascribed to the oxidation of methoxyhydroquinone and caffeic acid by comparison with their authentic voltammograms recorded under identical experimental conditions.

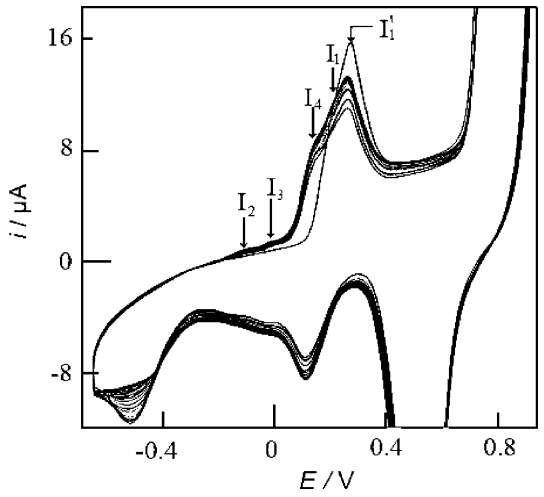

Fig. 8. Successive cyclic voltamograms of ferulic acid (0.5 mmol dm^{-3}) at gold disk in sulphuric acid aqueous solution at potential scan rate of 50 mV s^{-1}. Other conditions as in Figure 2.

3.1.7. *Oxidation mechanism of ferulic acid*

The results presented above suggest that ferulic acid molecules undergo a first electron transfer leading to the formation of phenoxy radicals for which the electronic charge distribution can be represented by four mesomeric forms **A**, **B**, **C** and **D** (Scheme 1). By considering the electronic effects of methoxy, carboxyvinyl and oxo groups, the radical **B** would be the most probable.

The formation of caffeic acid could be explained assuming that the radical **B** undergoes a second electron transfer leading to the carbocation **B′** which gives simultaneously the 3,4-dioxocinnamic acid (**E**, Scheme 2) and a methanol molecule by hydrolysis.

During the reverse scan, the 3,4-dioxocinnamic acid is reduced to caffeic acid (**F**, Scheme 2) at the potential of the reversible peak I_4.

Moreover, the proportions of ferulic acid oxidation products formed via the intermediary of the less probable forms **C** and **D** would be insignificant. The oxidation of radical **C** leads to the formation of methoxyparabenzoquinone (**G**, Scheme 3) which is reduced to methoxyhydroquinone (**H**, Scheme 3) at the potential of the reversible peak I_2.

The formation of 3,4-dihydroxy-5-methoxycinnamic acid (**I**, Scheme 4), stemming from the oxidation of the radical D, was not identified given that it is not commercial. However, the probable formation of this product could be supported by the comparison of its oxidation potential (peak I_3) with those of the methoxyhydroquinone (peak I_2) and caffeic acid (peak I_4). Taking into account the fact that the donating and attracting electronic effects displace the oxidation potential of hydroquinonic compounds towards the cathodic and anodic potentials respectively, the oxidation of the methoxyhydroquinone having a donating methoxy group would be easier than that of caffeic acid which possesses an attracting carboxyvinyl group. Therefore, the 3,4-dihydroxy-5-methoxycinnamic acid which has two attracting and donating groups must have an intermediate behaviour.

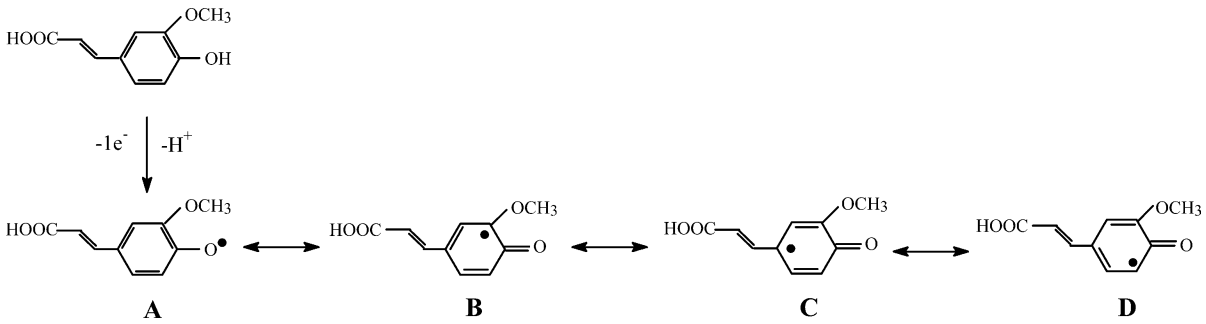

Scheme 1

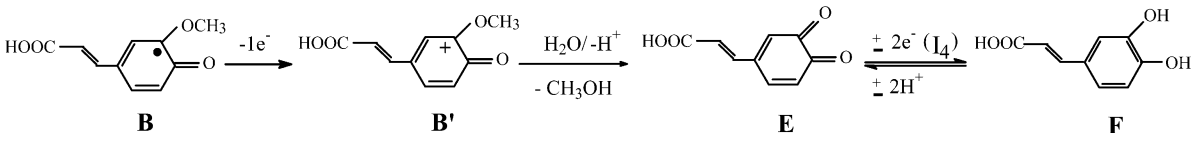

Scheme 2

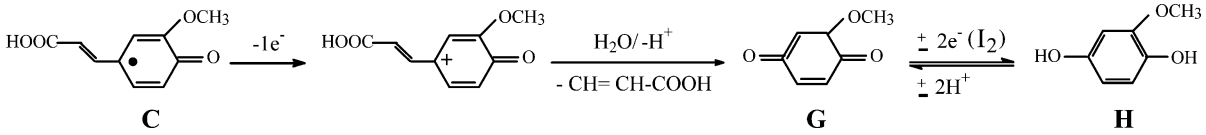

Scheme 3

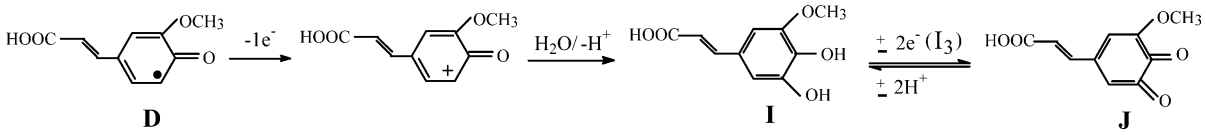

Scheme 4

3.2. *Degradation of ferulic acid on Ta/PbO₂ anode*

The total oxidation mechanism of ferulic acid was studied by monitoring its concentration and that of the main intermediate products during electrolysis of an aqueous solution (0.5 mmol dm^{-3}) on a Ta/PbO_2 anode. The amount of CO_2 formed is quantified from the total organic carbon value (TOC). The principal aromatic

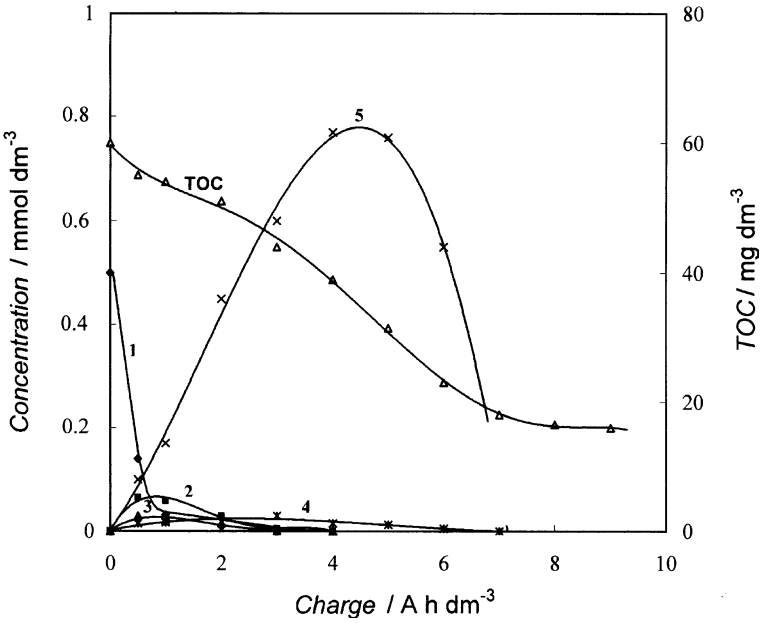

Fig. 9. Variation of the concentration of ferulic, caffeic, maleic, formic acids, methoxyhydroquinone and TOC during the electrolysis of ferulic acid aqueous solution (V = 140 cm^3) at Ta/PbO_2 anode (S = 10 cm^2). Initial ferulic acid concentration: 0.5 mmol dm^{-3}; anodic current density: 12 mA cm^{-2}; T = 65 °C; pH = 2. Key: (1) ferulic acid; (2) caffeic acid; (3) methoxyhydroquinone; (4) maleic acid; (5) formic acid; (TOC) total organic carbon.

compounds, identified by HPLC, are caffeic acid and methoxyhydroquinone. These results are in good agreement with the oxidation mechanism proposed from the cyclic voltammetry results. The other intermediate products identified are maleic acid, oxalic acid and formic acid.

The analysis of Figure 9 (curve1) shows that ferulic acid is oxidised according to a first order reaction. Thus, ferulic acid oxidation is limited by mass transport from the solution to the anode surface. The value of the apparent mass transfer coefficient, calculated as indicated in [9], is 7.9×10^{-5} m s^{-1}. Under the operating conditions of Figure 9, ferulic acid totally disappeared after passing a charge of 3 Ah dm^{-3}. During the electrolysis, the concentration of caffeic acid, maleic acid, oxalic acid and methoxyhydroquinone did not exceed 0.1 mmol dm^{-3} while that of formic acid reached 0.8 mmol dm^{-3}. Maleic acid and formic acid are formed independently via reaction of aromatic intermediates with hydroxyl radicals formed at the anode from water oxidation. Maleic acid proceeds from the breaking of benzenic rings and is oxidised to oxalic acid, which is very slowly transformed into CO_2 [25]. Figure 9 shows that, right from the beginning of the electrolysis, an instantaneous drop in the TOC value was observed. This indicates that CO_2 molecules are formed simultaneously with the other intermediates. Furthermore, the degree of TOC elimination, at the end of the electrolysis, is nearly equal to 80%.

4. Conclusion

The electrochemical oxidation of ferulic acid in water and in mixtures of water–acetone was studied by cyclic voltammetry as a function of various experimental parameters (ferulic acid concentration, volumetric fraction of acetone, potential scan rate and the charge Q characterizing the state of the treated gold surface).

The proposed mechanism is based on the discharge of a ferulic acid molecule in its free and adsorbed forms leading to three cations in which the charge distribution determines the amount of oxidation products. The hydrolysis of these cations leads to caffeic acid, methoxyhydroquinone and 3,4-dihydroxy-5-methoxycinnamic acid. The formation of caffeic acid and methoxyhydroquinone is confirmed from their authentic cyclic voltammograms.

Electrolysis of ferulic acid aqueous solution on a Ta/PbO_2 anode leads mainly to the formation of caffeic acid and methoxyhydroquinone as the first intermediates which are oxidised to maleic acid, oxalic acid and formic acid. The degradation of these three products leads to carbon dioxide and water. At the end of electrolysis the percentage of ferulic acid converted to CO_2 and H_2O is nearly 80%.

References

1. M. Hamdi, J.L. Garcia and R. Ellouz, *Bioprocess Eng.* **8** (1992) 79.
2. A. Cicheli and M. Solinas, *Riv. Merceol.* **23** (1984) 55.
3. F. Caruncio, C. Crescenzi, A.M. Girelli, A. Messina and A.M. Tarola, *Talanta* **55** (2001) 189.
4. J.B. Heredia, J. Torregrosa, J.R. Dominguez and J.A. Peres, *Chemosphere* **45** (2001) 85.
5. J.B. Heredia, J. Torregrosa, J.R. Dominguez and J.A. Peres, *Wat. Res.* **35** (2001) 1077.
6. M.A. Miranda, A.M. Amat and A. Arques, *Water Sci. Technol.* **44** (2001) 325.
7. P. Hapiot, A. Neudeck, J. Pinson, H. Fulcrand, P. Neta and C. Rolando, *J. Electroanal. Chem.* **405** (1996) 169.
8. B. Fleszar and J. Ploszynska, *Electrochim. Acta* **30** (1985) 31.
9. N. Belhadj Tahar and A. Savall, *J. Electrochem. Soc.* **145** (1998) 3427.
10. N. Belhadj Tahar and A. Savall, *J. Appl. Electrochem.* **29** (1999) 277.
11. L.L. Houk, S.K. Johnson, J. Feng, R.S. Houk and D.C. Johnson, *J. Appl. Electrochem.* **28** (1998) 1167.
12. V. Smithde Sucre and A.P. Watkinson, *Can. J. Chem. Eng.* **59** (1981) 52.
13. N. Belhadj Tahar and A. Savall, *J. New Mat. Electrochem. Syst.* **1** (1999) 19.
14. Ch. Comninellis and C. Pulgarin, *J. Appl. Electrochem.* **23** (1993) 108.
15. S. Stucki, R. Kötz, B. Carcer and W. Suter, *J. Appl. Electrochem.* **21** (1991) 99.
16. J. Iniesta, P.A. Michand, M. Panizza, G. Cerisola, A. Aldaz and Ch. Comninellis, *Electrochim. Acta* **46** (2001) 3573.
17. F. Montilla, P.A. Michaud, V. Morallon, J.L. Vasquez and Ch. Comninellis, *Electrochim. Acta* **47** (2002) 3509.
18. B. Boye, P.A. Michaud, B. Marselli, M.M. Dieng, E. Brillas and Ch. Comninellis, *New Diamond Frontier Carbon Technol.* **12** (2002) 63.
19. A. Kraft, M. Stadelmann and M. Blaschke, *J. Hazard. Mat.* **103** (2003) 247.
20. J.S. Clarke, R.E. Ehigamusoe and A.T. Kuhn, *J. Electroanal. Chem.* **70** (1976) 333.
21. S. Kallel Trabelsi, N. Belhadj Tahar and R. Abdelhedi, *Electrochim. Acta* **49** (2004) 1647.
22. R. Abdelhedi and M.L. Bouguerra, *Electrochim. Acta* **25** (1990) 273.
23. L.R. Sharma and R.K. Kalia, *Chem. Ind.* **20** (1975) 883.
24. M. Gattrell and D.W. Kirk, *J. Electrochem. Soc.* **140** (1993) 1534.
25. B. Boye, M.M. Dieng and E. Brillas, *Environ. Sci. Technol.* **36** (2002) 3030.